

Differences between CVID Granulomatosis and Sarcoidosis: Clinical, Immunological and Histopathological Comparison

Jean-François Viillard (✉ jean-francois.viillard@chu-bordeaux.fr)

University of Bordeaux II <https://orcid.org/0000-0001-7500-9323>

Maëlig Lescure

Eric Oksenhendler

Patrick Blanco

Jonathan Visentin

Marie Parrens

Research Article

Keywords: Hypogammaglobulinemia, Common variable immunodeficiency, Granulomatosis, STAT1, STAT3

Posted Date: May 18th, 2022

DOI: <https://doi.org/10.21203/rs.3.rs-1617117/v1>

License:  This work is licensed under a Creative Commons Attribution 4.0 International License.

[Read Full License](#)

Abstract

Common variable immunodeficiency granulomatous disease (CVID-GD) is a serious complication that occurs in 8–22% of CVID patients and can mimic sarcoidosis with which it shares certain clinical, biological and radiological features. However, no study to date has compared the two pathologies immunologically and histologically. Then, we analyzed the blood cell immunohistochemical-labeling profiles and the immunological-histological features of different biopsy samples from 10 patients with CVID-GD and compared them to those of with biopsy-proven sarcoidosis. Specifically, we wanted to know whether or not the signaling abnormalities observed in sarcoidosis granulomas are also present in CVID.

The CVID-GD immunological profile differs markedly from that of sarcoidosis, with a profound memory-cell deficit, strong CD8 + T-cell activation and altered balance in follicular helper-T cells (TFH) subsets in the blood. Morphological differences were found between CVID-GD histology and classical sarcoidosis, mainly the former's notable/extensive lymphoid hyperplasia associated with granulomas not observed in the latter. All organs involved with CVID-GD contained several TFH1 cells the granulomatosis, while TFH lymphocytes were inconstantly and more weakly expressed in sarcoidosis. Moreover, CVID and sarcoidosis granulomas expressed the signal transducer and activator of transcription (STAT)1 and STAT3 factors, regardless of the organ studied and without any significant difference between them. Our results suggest that the macrophage-activation mechanism in CVID resembles that of sarcoidosis, thereby suggesting that JAK-STAT-pathway blockade might be useful in currently difficult-to-treat CVID-GD.

Introduction

Common variable immunodeficiency (CVID), the most frequent symptomatic primary immune deficiency in adults, is characterized by hypogammaglobulinemia and recurrent infections, mainly of the respiratory tract, with encapsulated bacteria [1, 2]. Subjects with CVID may also develop non-infectious complications, including systemic granulomatous disease (GD) seen in 8–22% of patients with CVID (probably underestimated by the lack of histological evidence), that can markedly affect morbidity and mortality [3–6]. GD is diagnosed indifferently before or after CVID and, in the former context, often confused with sarcoidosis. The lungs are the prime site for granulomatous involvement, which is often associated with interstitial lymphocytic infiltration, and called granulomatous-lymphocytic interstitial lung disease (GLILD) [7]. However, about half of the patients have extrapulmonary GD mostly affecting lymph nodes, spleen and liver but other organs may be involved [8–11]. It is classically associated with autoimmunity, splenomegaly and severe deficiency of peripheral switched memory B lymphocytes [7].

While CVID-GD has been well-characterized clinically and distinguished from classical sarcoidosis [6, 11], the two entities' immunological and histological features were compared in only a few studies. We previously subjected 17 CVID patients' splenectomy samples to histological and phenotypic analysis and observed GD in nine, with a singular profile, i.e., granuloma often localized in the marginal zone, arranged in a rosary-bead pattern corresponding to granuloma distribution surrounding giant follicles, surrounded

by a majority of CD4⁺ T cells and a minority of CD8⁺ T cells, and associated with periarteriolar T-zone hyperplasia [12]. Those histological findings differ from those usually observed in sarcoidosis, i.e., diffusely distributed red-pulp granulomas. Those differences suggest that the two diseases are indeed different.

Herein, we compared the two entities to identify features suggestive of CVID when sarcoidosis-like granulomatosis was found. To try to discern clues about CVID-GD pathogenesis, we analyzed the histological and immunohistochemical profiles of different biopsy samples obtained from 10 CVID-GD patients and compared them to those of patients with biopsy-proven sarcoidosis. Specifically, we wanted to determine whether or not the signaling abnormalities observed in sarcoidosis granulomas are also present in CVID-GD.

Methods

Patients

All patients were recruited in the Department of Internal Medicine, Haut-Lévêque Hospital, University of Bordeaux, except two splenectomized-CVID patients enrolled in the French national DEFI cohort of adults with primary hypogammaglobulinemia [13]. These patients were registered in the ALTADIH study, which was approved by the Bordeaux University Hospital Ethics Committee (no. 2.04.2007). CVID was diagnosed using standard criteria [1]. Specifically, CVID diagnosis required (a) low serum IgG < 5 g/L combined with low IgM and/or IgA isotype concentrations < 0.4 or < 0.7 g/L, respectively; (b) poor antibody response to immunization or infection, and (c) exclusion of other defined forms of primary and secondary hypogammaglobulinemia. CVID-diagnosed patients' GD was defined as the presence of epithelioid and giant-cell granulomas in a biopsy of one or more tissue(s) or organ(s) taken from a patient with CVID. The biopsy was justified by clinical (e.g., skin nodules), biological (e.g., hepatic cytolysis) or radiological abnormalities (e.g., adenomegaly, splenomegaly). No genetic studies were performed on this cohort of patients. GD was diagnosed after excluding the differential diagnoses characterized by epithelioid and giganto-cellular granulomatous reactions.

Sarcoidosis patients were followed in the same department and diagnoses were based on the guidelines of the World Association of Sarcoidosis and Other Granulomatous Disorders [14]. All diagnoses were confirmed histologically in biopsies containing non-necrotizing epithelioid-cell-rich granulomas. CD4/CD8 ratios in 5 patients' bronchoalveolar lavage fluid (BALF) had > 3.5. Patients were retrospectively included in this study, selecting those with systemic sarcoidosis (more similar to disseminated forms of GD observed in CVID), available peripheral blood lymphocyte immunophenotyping at diagnosis and a remnant of their histological material at our hospital's Anatomopathology Department. Only 11 patients met those criteria. Retrospective non opposition to participate to the study was obtained from each individual.

For COVID patients, the following clinical information was recorded: sex, age at GD diagnosis, clinical splenomegaly, infections, autoimmune diseases, lymphoproliferation and enteropathy. For sarcoidosis patients, we listed the affected organs. For all patients, the following biological parameters were collected: hemogram values (neutrophils, hemoglobin, platelets), blood fibrinogen, C-reactive protein, aspartate aminotransferase, alanine aminotransferase, alkaline phosphatase, γ -glutamyltranspeptidase, calcemia, angiotensin-converting enzyme (ACE) and total gamma-globulin levels.

Flow-cytometry phenotypic analysis of blood B lymphocytes

For flow-cytometry analysis, blood was collected in EDTA and samples were analyzed within 24 hours. For B-cell phenotyping, whole-blood samples were labeled with fluorescent anti-CD19, anti-CD20, anti-CD27, anti-CD21 (all from Beckman Coulter, Brea, CA) and anti-IgD antibodies (BD Biosciences, San Diego, CA). Patients were then assigned to EURO-classes based on the absence or presence of circulating B lymphocytes (B^- : $\leq 1\%$ CD19⁺; B^+ : $>1\%$ CD19⁺ among total lymphocytes) [15]. B^+ patients were further classified according to the proportion of switched memory B (smB) cells (smB^- : $\leq 2\%$ IgD⁻CD27⁺/CD19⁺; smB^+ : $>2\%$ IgD⁻CD27⁺/CD19⁺).

For T-cell phenotyping, we used the following panel of monoclonal antibodies (mAbs): anti-CD45, -3, -4 and -8 (all from Beckman Coulter), and anti-HLA-DR (Beckman Coulter) as a T-lymphocyte-activation marker. To phenotype blood follicular helper-T cells (TFHs), whole blood samples were labeled with fluorescent anti-CD45, -CD3 and -CD4, -CD45RA (all from Beckman Coulter), anti-CXCR5, anti-CXCR3, anti-CCR6, anti-ICOS and anti-programmed cell-death protein-1 (PD-1) antibodies (all from BD Biosciences). Regulatory T-cell labeling were labeled with following panel of mAbs: fluorescent anti-CD4, -CD25, and -CD127 (all from Beckman Coulter). Natural killer (NK)/B-cells were labeled with the following panel of mAbs: anti-CD45, -56, -19, -3 and -CD16 (all from Beckman Coulter).

Red blood cells in all samples were lysed with Versalyse (Beckman Coulter). Absolute total lymphocyte counts were determined with Flow Count Fluorospheres (Beckman Coulter). NAVIOS flow-cytometer (Beckman Coulter) collected the data that were analyzed with Kaluza software (Beckman Coulter).

Results of 19 age-matched healthy donors (43 ± 16.4 years old) previously included in a study by our team [16] served as controls.

Specimen Collection

Histology

All samples were studied and stored in the Bordeaux University Hospital Pathology Department. The COVID patients' specimens were: 4 of 6 surgical splenectomy specimens with sufficient material, 1 ileocecal resection surgical specimen and biopsies: 2 liver, 2 bone marrow, 1 skin and 5 lymph node. Sarcoidosis-patient archived biopsy samples for comparison were: 4 mediastinal lymph-node, 3 bronchial, 3 liver-puncture, 2 skin, and 1 accessory salivary gland. No splenectomy specimens from sarcoidosis patients were available.

Specimens were formalin-fixed and paraffin-embedded (FFPE), and frozen tissue was available for 5. Hematoxylin – eosin (HE)-stained sections were subjected to histological reexamination in Haut-Lévêque Hospital. Specific staining (Ziehl–Neelsen for acid-fast bacilli and Gomori methenamine–silver for fungi) was done only for patients with necrotizing granulomas.

Tissue immunohistochemical (IHC) labeling

Leica BOND III IHC labeling was done according to the Leica IHC F protocol (Leica, Nanterre, France). The antibody panel included anti-PD-1 (NAT-105 BioSB, Blagnac, France), -ICOS CD278 (polyclonal antibody E18650, Spring Bioscience, Blagnac, France) and -CXCR3 (mAb clone 49801, R & D Systems, Lille, France), phosphorylated-signal transducer and activator of transcription (Phospho-STAT1 (Tyr701) (58D6) XP® Rabbit mAb, Cell Signaling Technology, Leiden, The Netherlands) and phosphorylated-STAT3 (Phospho-STAT3 (Tyr705) (D3A7) XP® Rabbit mAb, Cell Signaling Technology). Marker expression was analyzed in the granuloma histiocytes or lymphocytes. All 4/5 markers were scored as described previously by Furudoi et al. [12].

Statistical analyses

Median percentages and absolute cell counts were compared between groups with Mann-Whitney *U*-test; significance was defined as $P = 0.05$. Statistical analyses were computed with Statistica Inc. software (Statsoft, Tucson, AZ).

Results

Patient study groups

CVID patients

Among our 125 CVID-patient cohort followed in our department, 10 had biopsy-proven GD, all of them were enrolled in the ALTADIH Cohort (approved by the Bordeaux University Institutional Review Board on December 20, 2006). Their epidemiological and clinical characteristics are summarized in **Table 1**. These 6 men and 4 women had a mean age 46.6 (range, 18–69) years at the time of the GD diagnosis. All patients had recurrent bacterial infections (mostly pneumonia and sinusitis), but 8 experienced other non-infectious diseases frequently. Seven patients had multiple lymphadenopathies: 4 with histologically proven lymphoid hyperplasia (1 had GLILD). Among the 4 patients with autoimmune diseases, 2 had autoimmune thrombocytopenic purpura (ITP), 2 had Biermer's disease and 1 had autoimmune thyroiditis. Liver nodular regenerative hyperplasia (NRH) was found in 3 patients. Two patients had gastrointestinal disease with chronic diarrhea and villous atrophy. Among the 9 patients with splenomegaly, 6 were splenectomized; they were the subject of a previous publication [12]. Granulomas were seen in spleen, lymph nodes, bone marrow, liver, skin and gastrointestinal tract for 6, 5, 2, 2, 1 and 1 patients, respectively.

Baseline laboratory findings are reported in **Supplemental Table 1**. Serum IgG, IgA and IgM levels before replacement therapy were low: IgG (median: 1.23 [interquartile range (IQR): 0.84–3.83] g/L; normal range:

6.6–12.8 g/L), IgA (median: 0.025 [IQR: 0–0.07] g/L; normal range: 0.7–3.4 g/L) and IgM (median: 0.35 [IQR: 0.23–0.48] g/L; normal range: 0.5–2.1 g/L) (data not shown).

According to EURO-class [15], among the 10 CVID patients, only patient 6 had < 1% B cells among lymphocytes (B⁻ group). The 9 other patients with higher percentages (B⁺ group) were then categorized according to their class-switched memory B-cell (smB) status: 7 had severe smB deficiency (\leq 2% B cells (smB⁻) patients 1, 2, 4, 5, 7, 8 and 10) and patients 3 and 9 had > 2% (smB⁺). EURO-class also discriminates between patients according to CD21^{low} B-cell expansion: above or below 10% (CD21^{low} vs. CD21^{norm}). CD21 could not be evaluated for 4 CVID patients, while patients 1, 2, 5 and 9 were assigned to the CD21^{low} group.

Sarcoidosis patients

Among patients hospitalized for sarcoidosis during the last years, we selected 11 (6 men) with sarcoidosis involving at least 2 organs, immunophenotyping at diagnosis (including TFH cells) and for whom sufficient pathological material was available. Their demographic and clinical characteristics are summarized in **Table 2**. Their median age at diagnosis was 39 (range, 26–72) years. General signs were frequent: 3 were febrile, 3 had night sweats, 7 were asthenic and 4 had lost weight. At sarcoidosis diagnosis, patients had documented, in decreasing order of frequency, mediastinal lymphadenopathy in all, pulmonary interstitial syndrome in 8, subdiaphragmatic adenopathy in 3, arthritis in 5, hepatomegaly in 5, cardiac involvement in 2, peripheral neurological involvement in 2, and, in 1 each: central neurological involvement, renal involvement, bone involvement, splenomegaly or splenic nodules without splenomegaly. The pulmonary interstitial syndrome, characterized by computed-tomography (CT) scan, visualized: ground-glass images in 1, and micronodules with perilymphatic (in 3), central–lobular and peri-lymphatic (in 2), scissural (in 1) or ubiquitous (in 1) distributions.

Laboratory Findings: CVID vs. Sarcoidosis Patients

Laboratory results are reported in **Supplemental Table 1**. The two groups differed significantly for peripheral platelet counts, and ACE and total gamma-globulin levels. Thrombocytopenia was frequent in CVID-GD patients, but was absent in sarcoidosis patients, with respective medians of 137.5 G/L and 290.5 G/L ($P=0.0016$). All CVID-GD patients were always hypogammaglobulinemic whereas gamma-globulin levels were normal or increased in those with sarcoidosis: respective medians of 4 g/L and 13.2 g/L, respectively ($P<0.0001$). The ACE concentration was significantly more frequently elevated in CVID-GD patients, but the extreme values were more often observed in sarcoidosis patients whose levels could exceed 3× normal ($P<0.0001$).

Immunological Phenotypes: CVID vs. Sarcoidosis Patients

CVID-GD and sarcoidosis patients' blood-lymphocyte immunological marker values are reported in Table 3. Percentages of CD19⁺CD27⁻IgD⁺ naïve and CD19⁺CD27⁺IgD⁻ smB (smB⁻) B-cell subpopulations were significantly higher and lower, respectively, in CVID-GD than sarcoidosis patients ($P=10^{-3}$ and 10^{-4}).

Although no quantitative between-group differences were observed for the circulating T-cell compartment, CVID patients' median percentage of CD8⁺ T-lymphocytes was significantly higher than that of sarcoidosis patients ($P = 0.006$).

T-lymphocyte surface HLA-DR expression, reflecting their activation status, was examined on T-cell subsets. Comparing CVID-DG vs. sarcoidosis, CVID-GD patients had significantly higher percentages of HLA-DR-expressing T-CD3⁺ cells ($P = 0.003$), with overall significantly higher percentages of CD4⁺- and CD8⁺HLA-DR⁺ T cells with the latter largely predominating ($P = 0.05$ and 0.0009 , respectively). In sarcoidosis, similar percentages of CD4⁺- and CD8⁺HLA-DR⁺ T cells were activated.

Among the CD4⁺ T cells, we then focused on the TFH, which specialized B-cell helpers. As shown in Table 3 the TFH population accounted for a median of ~ 20% of the circulating CD4⁺ T cells in CVID patients, a rate significantly higher than in sarcoidosis patients ($P = 0.008$). TFH subpopulation analyses based on their CXCR3 and CCR6 expressions [16], circulating TFH1 cells (absolute count) predominated and, mostly, in frequency, in both populations but at a significantly higher percentage in CVID-GD patients ($P = 0.002$). Conversely, circulating TFH2 and TFH17 percentages were drastically lower than TFH1 in CVID-GD patients, and were significantly more represented in sarcoidosis patients ($P = 0.008$ and 0.004 , respectively). We did not observe TFH-subpopulation differences between sarcoidosis patients and healthy controls (data not shown).

Finally, CVID-GD patients had a significantly lower NK-cell levels than sarcoidosis patients ($P = 0.001$).

Histological and Immunohistochemical Findings: CVID-GD vs. Sarcoidosis Patients

Morphology

We clearly observed morphological differences between CVID-GD and classical sarcoidosis. For CVID patients, granulomas were most often epithelioid and giant-cell, non-necrotizing, variable in size from patient to patient and concentric in arrangement. As we had previously observed in the spleens of CVID patients [12], lymphoid hyperplasia frequently accompanies the granulomatous reaction, with epithelioid granulomas either arranged in a crown around a reactive follicle (Fig. 1A, adenopathy biopsy), either surrounded by a dense lymphocytic infiltrate (Fig. 2A, skin biopsy). In contrast, for sarcoidosis patients, as shown in Figs. 1B and 2B, the histological report revealed non-necrotizing epithelioid and giant-cell granulomas leaning against each other, focally encircled by fibrosis, with an inter-lesion parenchyma essentially formed of small mature lymphocytes. In each case, no lymphocytic reaction is described.

IHC labeling

Turpin et al. reported strong ratio of TFH1 lymphocytes (CXCR3 labeling) in CVID spleens [17]. We wanted to determine their presence in tissues other than the spleen and in another systemic granulomatosis, i.e., sarcoidosis. We confirmed the presence of several TFH cells, detected via PD-1-labeling, in all organs involved (lymph node, Fig. 1C; skin, Fig. 2C; bone marrow and liver, data not shown). Moreover, the observed CXCR3 labeling was in the same area of serial sections highlighting the presence of TFH1 cells. In contrast, TFH lymphocytes were seen less consistently and were less expressed in sarcoidosis patients, regardless of the tissue analyzed (Figs. 1D and 2D). Comparing scoring, TFH were significantly less expressed in sarcoidosis patients (Fig. 3A and 3B).

Moreover, it is well-documented that the Janus kinase (JAK)-STAT pathway is activated in sarcoidosis granulomas with an overexpression of STAT markers, mainly STAT1 but also STAT3. We then evaluated this metabolic pathway in CVID-GD. We observed that CVID and sarcoidosis granulomas similarly expressed the transcription factors STAT1 and STAT3, regardless of the organ studied (Figs. 1 and 2, E–F **and G–H**, respectively), but without any significant difference between them (Fig. 3C and 3D). STAT1-expression scores were comparable for CVID and sarcoidosis histiocytes (with or without epithelioid morphology) but the former was significantly higher than for CVID lymphocytes; sarcoidosis STAT1 also scored significantly higher on histiocytes than their lymphocytes (Fig. 3C). STAT3-expression was more ubiquitous (Fig. 3D). More qualitatively, we observed lost STAT3 expression when macrophages became epithelioid, i.e., in the center of the granuloma in both groups (Figs. 1 and 2, G–H).

Discussion

While the clinical, biological and radiological characteristics of several series of CVID–GD patients have been described [6, 8, 10], and even compared to those of classical sarcoidosis [18, 19], none has focused on the blood immunological phenotype and the histological differences between the two diseases. Because granulomatosis diagnosis may precede that of CVID, it is important for both clinicians and pathologists to have markers suggesting the possible CVID in the presence of granulomatosis. Hence, this work was undertaken to compare CVID-GD and sarcoidosis characteristics to identify features suggestive of CVID-GD, primarily searching for immunological and histological differences. For this purpose, we included all CVID patients, whose organ biopsies contained GD, and sarcoidosis patients, followed in our department, and who had available sufficient tissue material and retrospective blood lymphocyte immunophenotyping.

CVID-GD is characterized by non-caseating granulomas potentially involving any organ and occurs in 8–22% of CVID patients [3, 5, 10, 13], and 13.5% in the French DEFI cohort with slight female predominance [19]. In that cohort, the median age of GD onset was 40 years, and was most often diagnosed after CVID (median, 2.1 years later), although some cases may precede CVID development. Consanguinity, autoimmune cytopenias and splenomegaly were more frequent in CVID-GD patients than those without GD. The lung was the most prominent GD localization, although other extrathoracic organs were also

involved, mainly liver and spleen, more frequently than in sarcoidosis. Globally, although modest in size, our patient sample well reflects this clinical pattern.

Three laboratory parameters differed significantly between the two diseases: 1) blood platelet level was lower in CVID, probably because some patients also had ITP and others had splenomegaly; 2) ACE levels were higher in CVID, but no difference was observed in the Bouvry et al.'s larger cohort of [6], probably because high raised levels of ACE may be more documented in sarcoidosis; 3) and blood total gamma-globulin levels were dramatically higher in sarcoidosis. None of our patients had hypercalcemia.

Based on thoracic CT scans, Bouvry et al. [6] showed CVID lung involvement to be characterized by large randomly distributed nodules, preferentially localized in the lower lung zones, in the presence of air bronchograms and smooth margins surrounded by ground-glass opacities (halo sign) and bronchiectasis. Moreover, the usual micronodules distribution observed in sarcoidosis was significantly less frequent in CVID-GD than sarcoidosis (100% vs. 42%, respectively). We did not compare radiological profiles because sarcoidosis patients were not matched with CVID-GD patients for radiographic granulomatosis staging.

Notable immunological differences were found between CVID-GD and sarcoidosis patients. First, circulating naïve B-lymphocytes were significantly higher and circulating smB⁻ cells drastically lower. Previous study results showed a correlation between fewer peripheral smB⁻ cells and granulomatosis, especially when associated with splenomegaly [15, 20]. Although described in sarcoidosis vs. healthy controls [21], none of our patients with sarcoidosis has lower smB⁻ cell counts. The lowest percentage of smB⁻ cells in our sarcoidosis patients always remains higher than the highest percentage observed in CVID patients. Second, the percentage of activated, blood T lymphocytes (predominantly CD8⁺) was significantly higher in CVID than sarcoidosis, which was characterized by comparably lower percentages of CD4⁺ and CD8⁺ subpopulations. In this study, we established a strong association between CVID-GD and increased CD8⁺ T-cell activation, thereby consolidating the important link between T-cell activation and clinical complications we previously assessed [22]. Third, we confirmed elevated blood TFH cells in CVID-GD patients, with a skewing toward TFH1 cells in contrast to TFH2 and TFH17 populations, while peripheral TFH-subpopulation distributions of healthy controls and sarcoidosis patients did not differ. We previously showed an inverse correlation between circulating TFH1 and smB⁻ cells, mainly in CVID patients with non-infectious complications including GD [17]. Thus, the immunological profile of CVID-GD patients differs markedly from that of sarcoidosis patients, with a profound memory-cell deficit, strong CD8⁺ T-cell activation and altered TFH-subset balance in blood.

CVID GD morphology from patients differ from that of sarcoidosis. Granulomas in the latter are often uniform in appearance, non-necrotizing, tend to become confluent adjacent to each other and, in older cases, exhibit a peripheral rim of hyalinization or fibrosis [23]. In CVID, granulomas vary in size, are arranged concentrically, either in a crown around a reactive follicle or surrounded by a dense lymphocytic infiltrate. This lymphoid proliferation is not observed in sarcoidosis. We previously described this

histological pattern in the spleens of several CVID patients [12], but showed herein that it also concerns other organs, such as lymph nodes and skin. These features should alert the pathologist analyzing granuloma to suggest a CVID-like disease. Moreover, we previously described an accumulation of TFH1 cells in the spleen of CVID patients [17], and confirmed that observation herein; moreover, TFH1 cells were also seen in other tissues with GD, e.g., skin or lymphadenopathy. That represents a notable distinction with sarcoidosis.

Finally, granuloma-formation processes in CVID remain unelucidated and it is unknown whether they resemble those in sarcoidosis. Several groups demonstrated constitutively upregulated JAK-STAT–signaling in sarcoidosis, attributed to increased production of cytokines, mainly interferon-gamma (IFN- γ) by T lymphocytes [24–26]. The results of several studies on sarcoidosis showed constitutive activation of JAK-STAT–signaling at the messenger RNA level in peripheral blood mononuclear cells and other tissues, and found constitutive activation of STAT1 and STAT3 proteins in granulomas [25, 27]. To determine whether the same pattern occurred in the CVID granuloma, we undertook IHC-labeling studies on different archival tissue samples to assess activated JAK-STAT signaling (with p-STAT1 and p-STAT3). As in sarcoidosis, CVID granuloma exhibited a similar pattern of p-STAT1 and p-STAT3 activation. Therefore, this constitutive activation of the JAK-STAT pathway may be a conserved feature of granulomatous disorders. These results suggest that JAK-STAT–pathway inhibition could be a promising therapeutic approach for CVID-GD patients, as recently reported for several cases of refractory sarcoidosis, including long-standing multiorgan disease, which had been successfully treated with the oral JAK (JAK1 and JAK3) inhibitor tofacitinib [27–29]. Corticosteroids are the gold-standard therapy for CVID-GD, but complete response is infrequent and their long-term side effects preclude their long-term use. Other immunosuppressive drugs have been used with varying degrees of efficacy but no therapeutic combination has demonstrated superiority, although rituximab is commonly used prescribed for associated lymphoproliferation. Thus, tofacitinib efficacy and safety in CVID-GD patients should be evaluated.

We are well-aware that our study has several limitations. Our patient sample is small but CVID-GD remains a rare disease for which it is difficult to recruit many patients. Our control population was arbitrary and we selected only patients admitted to our department for sarcoidosis, with sufficient tissue material available, several organs affected to closely resemble the systemic form, and retrospective immunological phenotyping, criteria not met by our entire sarcoidosis cohort. However, this selected group reflects the heterogeneity of the sarcoidosis. The differences observed between the two study populations seem homogeneous despite the small number of patients.

In conclusion, our results established several differences between CVID-GD and sarcoidosis, some of which had never been reported previously, mainly in terms of histology, allowing a pathologist to evoke CVID-GD in the presence of tissue granulomatosis. Nevertheless, the mechanism of macrophage activation seems to be the same as in sarcoidosis, suggesting possible use of agents blocking the JAK-STAT pathway in CVID-GD, which remains difficult-to-treat.

Declarations

Author Contributions JFV, ML and EO enrolled CVID patients in the cohort and collected clinical data. PB and JV ran the flowcytometric analyses. ML and MP conducted the histological analyses and tissue immunohistochemical labeling. ML computed the statistical analyses of the data. MP created the histological figures. JFV and MP wrote the paper.

Funding. This study was carried out with the Internal Medicine Department's own funds.

Data Availability. Not applicable.

Ethics Approval and Consent to Participate. CVID patients were enrolled in the ALTADIH Cohort which was approved by the Bordeaux University Institutional Review Board on December 20th, 2006 (n°2.04.2007). Each CVID patient gave informed written consent before participating in the study. Informed consent was obtained from sarcoidosis patients.

Consent for Publication. The patient consent form contains permission to publish data without an identifier.

Conflict of Interest The authors declare no conflict of interest.

References

1. Picard C, Al-Herz W, Bousfiha A, Casanova JL, Chatila T, Conley ME, et al. Primary immunodeficiency diseases: an update on the classification from the International Union of Immunological Societies Expert Committee for primary immunodeficiency 2015. *J Clin Immunol.* 2015;35:696–726.
2. Kobrynski L, Powell RW, Bowen S. Prevalence and morbidity of primary immunodeficiency diseases, United States 2001–2007. *J Clin Immunol.* 2014;34(8):954–61.
3. Chapel H, Lucas M, Lee M, Bjorkander J, Webster D, Grimbacher B, et al. Common variable immunodeficiency disorders: division into distinct clinical phenotypes. *Blood.* 2008;112:277–86.
4. Resnick ES, Moshier EL, Godbold JH, Cunningham-Rundles C. Morbidity and mortality in common variable immune deficiency over 4 decades. *Blood;* 2012;119:1650–7.
5. Ho HE, Cunningham-Rundles C. Non-infectious complications of common variable immunodeficiency: updated clinical spectrum, sequelae, and insights to pathogenesis. *Front Immunol.* 2020;11:149. doi: 10.3389/fimmu.2020.00149.
6. Bouvry D, Mouthon L, Brillet P-Y, Kambouchner M, Ducroix J-P, Cottin V, et al. Granulomatosis-associated common variable immunodeficiency disorder: a case-control study versus sarcoidosis. *Eur Respir J.* 2013;41(1):115–22.
7. Mannina A, Chung JH, Swigris JJ, Solomon JJ, Huie TJ, Yunt ZX, et al. Clinical predictors of a diagnosis of common variable immunodeficiency-related granulomatous-lymphocytic interstitial lung disease. *Ann Am Thorac Soc.* 2016;13(7):1042–9.

8. Mechanic LJ, Dikman S, Cunningham-Rundles C. Granulomatous disease in common variable immunodeficiency. *Annals of Internal Medicine*. 1997;127(8):613–7.
9. Morimoto Y, Routes JM. Granulomatous disease in common variable immunodeficiency. *Curr Allergy Asthma Rep*. 2005;5(5):370–5.
10. Ardeniz Ö, Cunningham-Rundles C. Granulomatous disease in common variable immunodeficiency. *Clin Immunol*. 2009;133(2):198–207.
11. Boursiquot JN, Gérard L, Malphettes M, Fieschi C, Galicier L, Boutboul D, et al. Granulomatous disease in CVID: retrospective analysis of clinical characteristics and treatment efficacy in a cohort of 59 patients. *J Clin Immunol*. 2013;33(1):84–95.
12. Furudoï A, Gros A, Stanislas S, Hamidou M, Furudoï E, Oksenhendler E, et al. Spleen histologic appearance in common variable immunodeficiency: analysis of 17 cases. *Am J Surg Pathol*. 2016;40(7):958–67.
13. Oksenhendler E, Gerard L, Fieschi C, Malphettes M, Mouillot G, Jaussaud R, et al. Infections in 252 patients with common variable immunodeficiency. *Clin Infect Dis*. 2008;46(10):1547–54.
14. Statement on sarcoidosis. Joint statement of the American Thoracic Society (ATS), the European Respiratory Society (ERS) and the World Association of Sarcoidosis and Other Granulomatous Disorders (WASOGD) adopted by the ATS Board of Directors and by the ERS Executive Committee. *Am. J. Respir. Crit. Care Med*. 1999;160(2):736–755.
15. Wehr C, Kivioja T, Schmitt C, Ferry B, Witte T, Eren E, et al. The EUROclass trial: defining subgroups in common variable immunodeficiency. *Blood*. 2008;111(1):77–85.
16. Morita R, Schmitt N, Bentebibel SE, Ranganathan R, Bourdery L, Zurawski G, et al. Human blood CXCR5(+)CD4(+) T cells are counterparts of T follicular cells and contain specific subsets that differentially support antibody secretion. *Immunity*. 2011;34:108–21
17. Turpin D, Furudoï A, Parrens M, Blanco P, Viallard JF, Duluc D. Increase of follicular helper T cells skewed toward a Th1 profile in CVID patients with non-infectious clinical complications. *Clin Immunol*. 2018;197:130–8.
18. Arnold DF, Arnold DF, Wiggins J, Cunningham-Rundles C, Misbah SA, Chapel HM. Granulomatous disease: distinguishing primary antibody disease from sarcoidosis. *Clin Immunol*. 2008;128:18–22.
19. Boursiquot JN, Gérard L, Malphettes M, Fieschi C, Galicier L, Boutboul D, et al. Granulomatous disease in CVID: retrospective analysis of clinical characteristics and treatment efficacy in a cohort of 59 patients. *J Clin Immunol*. 2013;33:84–95.
20. Picat MQ, Thiébaud R, Lifermann F, Delbrel X, Adoue D, Wittkop L, et al. T-cell activation discriminates subclasses of symptomatic primary humoral immunodeficiency diseases in adults. *BMC Immunol*. 2014;15:13. doi: 10.1186/1471-2172-15-13
21. Lee NS, Barber L, Akula SM, Sigounas G, Kataria YP, Arce S. disturbed homeostasis and multiple signaling defects in the peripheral blood B-cell compartment of patients with severe chronic sarcoidosis. *Clin Vaccine Immunol*. 2011;18:1306–16.

22. Viillard JF, Ruiz C, Guillet M, Pellegrin JL, Moreau JF. Perturbations of the CD8(+) T-cell repertoire in COVID patients with complications. *Results Immunol.* 2013;29;3:122–8.
23. Rosen Y. Pathology of granulomatous pulmonary diseases. *Arch Pathol Lab Med.* 2022;146:233–51.
24. Rosenbaum JT, Pasadhika S, Crouser ED, Choi D, Harrington CA, Lewis JA, et al. Hypothesis: sarcoidosis is a STAT1-mediated disease. *Clin Immunol.* 2009;132:174–83.
25. Zhou T, Casanova N, Pouladi N, Wang T, Lussier Y, Knox KS, Garcia JGN et al. Identification of JAK-STAT signaling involvement in sarcoidosis severity via a novel microRNA-regulated peripheral blood mononuclear cell gene signature. *Sci Rep.* 2017;7:4237. doi: 10.1038/s41598-017-04109-6.
26. Li H, Zhao X, Wang J, Zong M, Yang H. Bioinformatics analysis of gene expression profile data to screen key genes involved in pulmonary sarcoidosis. *Gene.* 2017;596:98–104.
27. Damsky W, Thakral D, Emeagwali N, Galan A, King B, Damsky W, et al. tofacitinib treatment and molecular analysis of cutaneous sarcoidosis. *N Engl J Med.* 2018;379:2540–6.
28. Damsky W, Young BD, Sloan B, Miller EJ, Obando JA, King B, Damsky W, et al. Treatment of multiorgan sarcoidosis with tofacitinib. *ACR Open Rheumatol.* 2020;2:106–9.
29. Talty R, Damsky W, King B. Treatment of cutaneous sarcoidosis with tofacitinib: a case report and review of evidence for Janus kinase inhibition in sarcoidosis. *JAAD Case Rep.* 2021;16:62–4.

Tables

Table I: Summary of the demographic and clinical characteristics of COVID patients.

| Patients No. | Age ^a /Sex | Alive or deceased | Clinical manifestations ^b | Splenomegaly | Organs histologically affected by granulomatosis |
|--------------|-----------------------|-------------------|--|--------------|--|
| 1 | 53/M | Alive | Varicella-zoster infections, S,P, multiple lymphadenopathy | Yes | Skin, lymphadenopathy, bone marrow |
| 2 | 54/F | Dead | P, B, S, multiple lymphadenopathy | Yes | Spleen, lymphadenopathy |
| 3 | 69/M | Dead | S, B, P | Yes | Bone marrow |
| 4 | 36/M | Dead | S, P, B, NRH, ITP, multiple lymphadenopathy | Yes | Spleen |
| 5 | 22/M | Alive | S, B, P, multiple lymphadenopathy, lymphoid proliferation, GLILD | Yes | Spleen, lymphadenopathy, liver, digestive tract |
| 6 | 53/F | Alive | B, P, S, Warts, multiple lymphadenopathy, lymphoid proliferation, NRH | Yes | Spleen |
| 7 | 50/F | Alive | B, P, S, M, pernicious anemia, thyroiditis, lymphoid proliferation, villous atrophia | Yes | Spleen |
| 8 | 49/M | Alive | B, P, S, pernicious anemia, multiple lymphadenopathy, villous atrophia | Yes | Spleen, lymphadenopathy |
| 9 | 18/M | Alive | S, B, P | No | Lymphadenopathy |
| 10 | 62/F | Dead | S, P, B, NRH, ITP, multiple lymphadenopathy, lymphoid proliferation | Yes | Liver |

^aAge at biopsy identifying granulomatosis.

^bClinical manifestations observed throughout the course of the disease for each patient: B: Bronchitis; GLILD: Granulomatous-Lymphocytic Interstitial Lung Disease; ITP: Idiopathic Thrombocytopenic Purpura; NRH: Nodular Regenerative Hyperplasia; M: meningitis; P: Pneumonia; S: Sinusitis.

Table II: Summary of the demographic and clinical characteristics of sarcoidosis patients.

| Patients No. | Age ^a /Sex | Lymph node involvement | Pulmonary involvement ^b | Other organ involvement | Organs histologically affected by granulomatosis |
|--------------|-----------------------|------------------------|------------------------------------|--|--|
| 1 | 31/F | Yes | No | Skin, arthritis | Skin |
| 2 | 49/M | Yes | Yes | Salivary glands, arthritis | Accessory salivary gland |
| 3 | 29/F | Yes | Yes | Cranial neuropathy (facial palsy) | Adenopathy |
| 4 | 48/M | Yes | Yes | Cranial neuropathy (nerves VII, VIII), liver, arthritis | Adenopathy |
| 5 | 75/F | Yes | Yes | Heart | Bronchial mucosa |
| 6 | 33/M | Yes | Yes | Liver | Liver, bronchial mucosa |
| 7 | 35/M | Yes | No | Skin, arthritis | Skin |
| 8 | 48/F | Yes | Yes | Liver, spleen, heart, Central nervous system (spinal cord), bone | Bronchial mucosa |
| 9 | 23/F | Yes | No | Extra-pulmonary lymphadenopathies | Adenopathy |
| 10 | 36/M | Yes | Yes | Kidney, liver, arthritis | Liver |
| 11 | 46/M | Yes | Yes | Liver, spleen | Adenopathy, Liver |

^aAge at biopsy identifying granulomatosis. ^bA patient is considered to have lung involvement when lung parenchymal lesions are observed on CT scan (ground glass, micronodules of peri-lymphatic distribution, fibrosis for example).

Table 3. Immunological markers values of CVID and sarcoidosis patients.

| Parameters | CVID patients, <i>n</i> = 10 | Sarcoidosis patients, <i>n</i> = 11 | <i>P</i> value |
|---|-----------------------------------|--------------------------------------|----------------|
| Total circulating lymphocytes, /mm³ | 801 (473–3985) [276–3985] | 1027 (775–1692) [379–2538] | 0.511 |
| B cells | | | |
| CD19 ⁺ , cells/mm ³ | 103.5 (38–135) [0–379] | 118 (96–224) [46–433] | 0.314 |
| CD27 ⁻ IgD ⁺ , % CD19 ⁺ | 92.68 (87.15–94.85) [84.21–96.60] | 73.945 (68.265–82.745) [40.23–92.86] | 0.001 |
| CD27 ⁻ IgD ⁻ , % CD19 ⁺ | 1.45 (0.83–3.815) [0.44–5] | 2.055 (1.15–4.845) [0.47–41.12] | 0.645 |
| CD27 ⁺ IgD ⁺ , % CD19 ⁺ | 3.9 (1.835–9.215) [1.05–10.33] | 9.715 (6.815–15.46) [2.44–22.44] | 0.04 |
| CD27 ⁺ IgD ⁻ , % CD19 ⁺ | 1.33 (0.435–2.075) [0.08–3.38] | 9.605 (6.19–11.95) [3.73–12.62] | 0.0001 |
| T cells | | | |
| CD3 ⁺ , cells/mm ³ | 667.5 (392–1092) [224–2431] | 779 (439–1076) [243–1845] | 0.91 |
| CD4 ⁺ , cells/mm ³ | 393.5 (256–485) [109–1105] | 562 (323–747) [137–963] | 0.31 |
| % lymphocytes | 44.35 (39.64–50.74) [12–76.36] | 47.11 (36.75–54.14) [23.65–55.53] | 0.86 |
| CD8 ⁺ , cells/mm ³ | 249 (108–402) [30–1913] | 186 (104–311) [78–777] | 0.46 |
| % lymphocytes | 29.69 (23.36–37.69) [6.42–48] | 18.06 (14.85–20.58) [11.98–30.62] | 0.006 |
| Regulatory T cells, /mm³ | 44.5 (34–47) [24–49] | 54 (30–60) [26–64] | 0.16 |
| Activated T cells | | | |
| CD3 ⁺ HLA-DR ⁺ , % CD3 ⁺ | 37.45 (24.995–51.53) [8.12–57.39] | 10.67 (7.52–14.26) [5.3–25.74] | 0.003 |
| CD4 ⁺ HLA-DR ⁺ , % CD4 ⁺ | 40.50 (22.59–56.38) [4.7–65.13] | 17.65 (12.38–19.19) [7.12–47.77] | 0.05 |
| CD8 ⁺ HLA-DR ⁺ , % CD8 ⁺ | 61.035 (52.9–73) [19.4–95.38] | 18.27 (13.42–26.05) [6.99–34.65] | 0.0009 |
| Natural killer cells, /mm³ | 40 (28–131) [20–1092] | 141.5 (118–261) [86–333] | 0.05 |
| TFH lymphocytes, /mm³ | 71.5 (48–102) [24.41–134] | 61 (42.80–63.70) [38.5–86.73] | 0.39 |
| | 20.6 (12.16–23.57) | 11.13 (9.45–12.02) [6.31– | 0.008 |

| | | | |
|-----------------------------------|---------------------------------------|---------------------------------------|--------------|
| % LT CD4 ⁺ lymphocytes | [12.06–32.13] | 12.21] | |
| TFH1, /mm ³ | 52.29 (39.89–87.94) [22.03–120.48] | 26.56 (13.93–27.99) [13.86– 41.51] | 0.04 |
| % TFH | 86.92 (82.27–89.91) [59.54–90.25] | 42.55 (36.01–46.03) [32.55– 47.86] | 0.002 |
| TFH2, /mm ³ | 5.19 (3–7) [0.74–11.27] | 15.17 (9.95–16.62) [7.81– 18.67] | 0.004 |
| % TFH | 5.85 (3.05–8.85) [3.02– 16.82] | 24.88 (18.27–29.31) [11.48– 43.16] | 0.008 |
| TFH17, /mm ³ | 7.2 (3–9) [1.61–9.47] | 19.24 (16.97–21.06) [7.79– 35.19] | 0.008 |
| % TFH | 7.3 (6.88–8.87) [6.62– 23.16] | 30.85 (27.92–40.57) [20.23– 49.22] | 0.004 |

Results are expressed as medians, (25th–75th percentiles) and [ranges].

Comparisons were made with the non-parametric Mann–Whitney *U*-test. Significant values are in bold type.

Figures

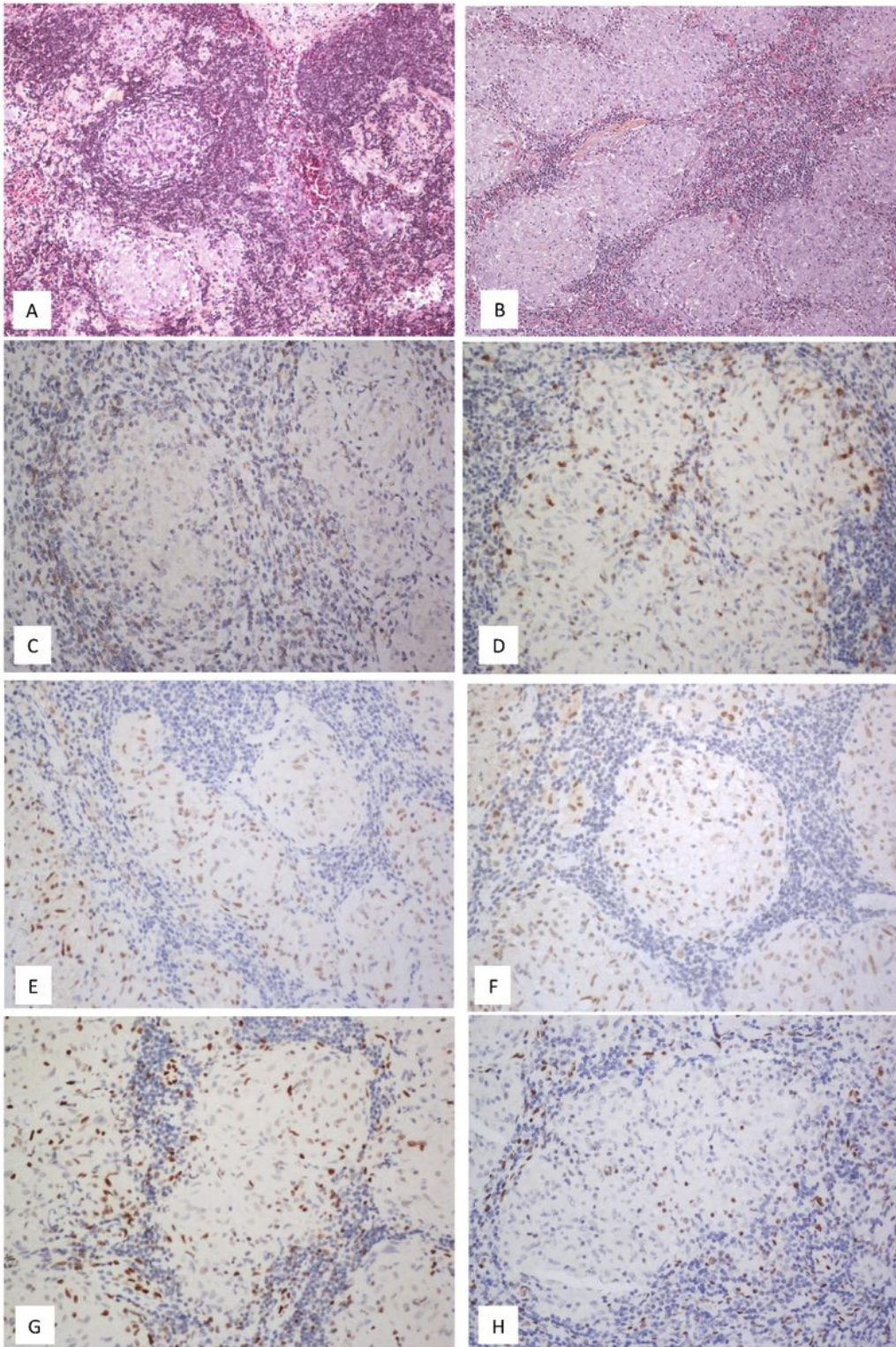


Figure 1

Lymph-node biopsies: left column: CVID; right column: sarcoidosis. **A.** Epithelioid granulomas arranged in a crown around a reactive follicle. Hematoxylin & eosin (HE) $\times 100$. **B.** Closely packed epithelioid granulomas focally surrounded by fibrosis. HE $\times 100$. **C–D.** C: score 4 (40–59%) PD-1-positive lymphocytes contrasting with a score 2 (5–19%) (D). HE $\times 200$. **E–F.** Phosphorylated signal transducer and activator of transcription (STAT)1 IHC labeling shows histiocyte nuclear positivity with or without

epithelioid morphology. HE x200. **G–H.** Phosphorylated STAT3 IHC labeling shows lymphocyte and histiocyte nuclear positivity, respectively, within and outside the granulomas, and without epithelioid morphology. HE ×200.

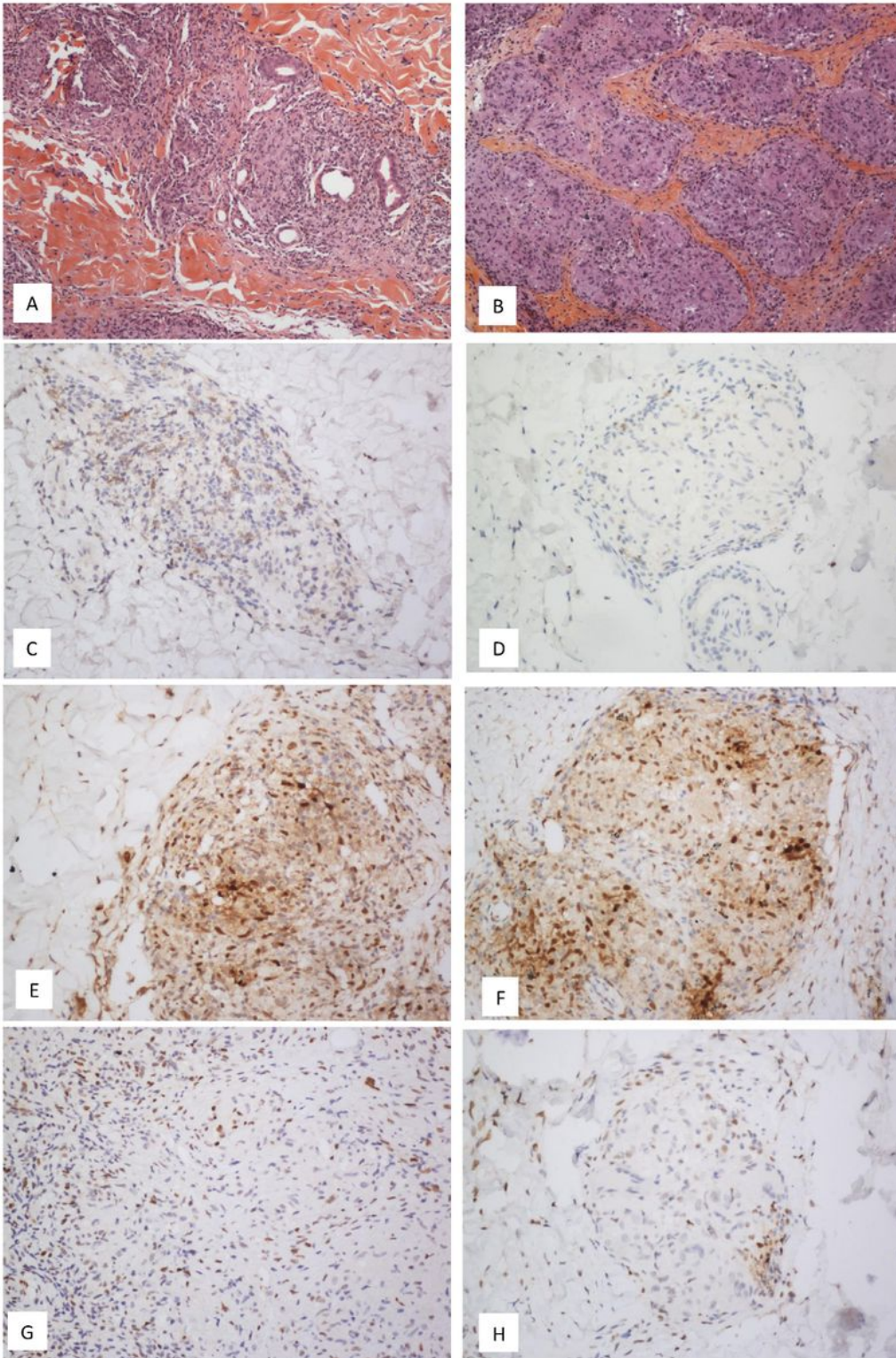


Figure 2

Skin biopsies: left column: CVID; right column: sarcoidosis. **A.** Histiocytic granulomas admixed and surrounded by a dense infiltrate composed of small mature lymphocytes. HE $\times 100$. **B.** Closely packed epithelioid granulomas surrounded by fibrosis. HE $\times 100$. **C–D.** C: score 4 (40–59%) PD-1-positive lymphocytes contrasting with a score 2 (5–19%) (D). HE $\times 200$. **E–F.** STAT1 IHC labeling shows histiocyte nuclear positivity with or without epithelioid morphology. HE $\times 200$. **G–H.** Phosphorylated STAT3 IHC labeling shows lymphocyte and nuclear positivity, respectively, within and outside the granulomas, and without epithelioid morphology. HE $\times 200$.

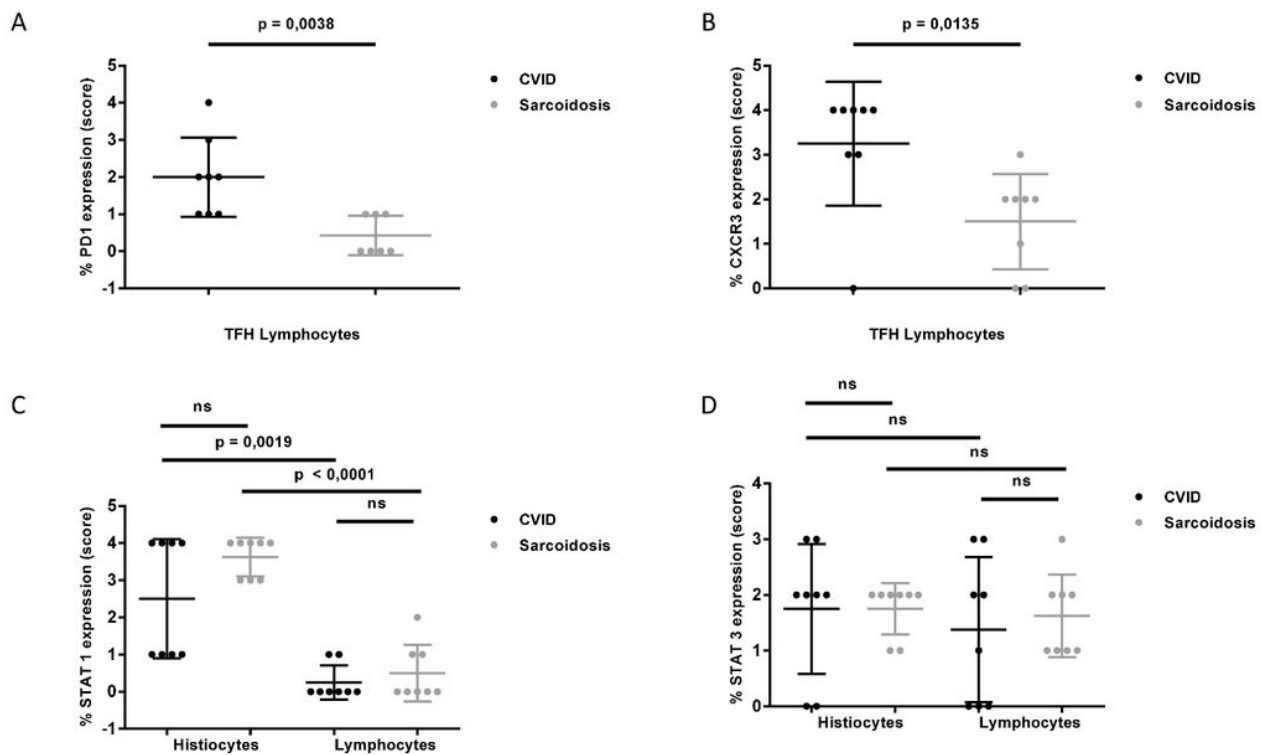


Figure 3

Cumulative immunohistochemical (IHC) labeling of **A** PD-1 and **B** CXCR3 in lymphocytes, and **C** phosphorylated STAT1 and **D** phosphorylated STAT3 in lymphocytes and histiocytes from 10 CVID patients and 11 sarcoidosis patients. The score is based on the percentage of positive (labeled) cells, defined as 0 (<1%), 1 ($\geq 1\%$ to <5%), 2 ($\geq 5\%$ to <20%), 3 ($\geq 20\%$ to <40%) and 4 ($\geq 40\%$ to <59%).

Supplementary Files

This is a list of supplementary files associated with this preprint. Click to download.

- [SupplementalTable1.docx](#)